In vitro exposure of leukocytes to HIV pre-exposure prophylaxis (PrEP) decreases mitochondrial function and alters gene expression profiles.

Emily R. Bowman[1], Cheryl Cameron[2], Brian Richardson[2], Manjusha Kulkarni[1], Janelle Gabriel[1], Aaren Kettelhut[1], Lane Hornsby[1], Jesse J. Kwiek[1], Abigail Norris Turner[1], Carlos Malvestutto[1], Jose Bazan[1], Susan L. Koletar[1], Susanne Doblecki-Lewis[3], Michael M. Lederman[2], Mark Cameron[2], Nichole R. Klatt[4], Jordan E. Lake[5], Nicholas T. Funderburg[1]

[1]The Ohio State University, Columbus, Ohio, USA; [2]Case Western Reserve University, Cleveland, OH, USA; [3]University of Miami, Miami, FL, USA; [4]Department of Surgery, University of Minnesota, Minneapolis, MN, USA; [5]The University of Texas Health Science Center, Houston, TX, USA

Running Title: PrEP alters immune cell function

Keywords: pre-exposure prophylaxis, mitochondrial dysfunction, leukocytes, lipids, inflammation, human immunodeficiency virus

Corresponding Author
Emily Bowman
333 W. 10th Ave.
5198 Graves Hall
Columbus OH, 43210
Phone: 614 292-1483
Email: Emily.Bowman@osumc.edu

Total Word Count: 4250
Total Abstract Count: 250

30 Number of Inserts: 7 Figures, 4 Supplemental Figures and Tables

31 Number of References: 57

Abstract

Background: The use of antiretroviral therapy (ART) as pre-exposure prophylaxis (PrEP) is an effective strategy for preventing HIV acquisition. The cellular consequences of PrEP exposure, however, have not been sufficiently explored to determine potential effects on health in individuals without HIV.

Methods: Peripheral blood mononuclear cells (PBMCs) from people without HIV were exposed to tenofovir disoproxil fumarate (TDF) or emtricitabine (FTC) overnight. Mitochondrial mass and function were measured by flow cytometry and Agilent XFp analyzer. Monocyte-derived macrophages (MDMs) were differentiated in 20% autologous serum for 5 days in the presence or absence of TDF or FTC, and surface markers, lipid uptake, and efferocytosis were measured by flow cytometry. MDM gene expression was measured using RNAseq. Plasma lipids were measured using mass spectrometry.

Results: PBMCs exposed to TDF or FTC had decreased maximal oxygen consumption rate (OCR) and reduced mitochondrial mass. Exposure to PrEP also increased reactive oxygen species (ROS) production from monocyte subsets. Compared to MDMs cultured in medium alone, cells differentiated in the presence of TDF (829 genes) or FTC (888) genes had significant changes in gene expression. Further, PrEP-exposed MDMs had decreased mitochondrial mass, and displayed increased lipid uptake and reduced efferocytosis. Plasma biomarkers and lipid levels were also altered *in vivo* in individuals receiving a PrEP regimen.

Conclusions: Exposure of leukocytes to TDF or FTC resulted in decreased mitochondrial function, and altered functional and transcriptional profiles. These findings may have important implications for the metabolic and immunologic consequences of PrEP in populations at risk for HIV acquisition.

Introduction

Eradication of human immunodeficiency virus (HIV) is a global priority, and use of pre-exposure prophylaxis (PrEP) to limit acquisition of new infections is an important strategy to achieve this goal(1). PrEP is effective at preventing HIV transmission(2), but exposure to antiretroviral therapy (ART) is not without consequences. Few studies, however, have investigated the potential off-target effects of PrEP use in people without HIV. The main FDA-approved form of PrEP is co-formulated tenofovir disoproxil fumarate (TDF) and emtricitabine (FTC) (Truvada®) taken once daily. Previous work has demonstrated that ART drugs, including nucleoside reverse transcriptase inhibitors (NRTIs), can decrease mitochondrial function(3, 4). Newer NRTIs, including TDF and FTC, are likely less toxic to mitochondria than older drugs (e.g. stavudine, didanosine), but TDF and FTC may also induce mitochondrial dysfunction, potentially through inhibition of mitochondrial DNA polymerase-γ and subsequent decreases in mitochondrial DNA (mtDNA) content and respiratory chain function(4-6). Mitochondrial dysfunction may result in changes in fatty acid oxidation (FAO)(7) and adipokine levels(8), thereby contributing to adipose tissue dysfunction and circulating lipid profile disturbances, and plausibly to increased cardiovascular disease (CVD) risk. Mitochondrial dysfunction may also contribute to local and systemic inflammation through mechanisms related to reactive oxygen species (ROS) production, NFκB signaling, and inflammasome activation(9). Many of the current studies exploring the effects of ART drugs on cellular mitochondrial function or lipid profiles are performed in people with HIV (PWH), and the inflammatory, immunologic, and metabolic complications associated with the complex pathophysiologic disturbances of HIV infection likely complicate the measurement of the direct effects of ART drugs on cellular function.

Here, we explore the potential functional and phenotypic consequences of *in vitro* exposure of TDF and FTC on peripheral blood mononuclear cells (PBMCs). We also evaluated

alterations in lipid profiles and plasma inflammatory biomarkers in a convenience cohort of people initiating PrEP. Our work suggests that exposure of immune cells to PrEP drugs could have unintended adverse effects on cellular function that may contribute to altered innate immune responses and, potentially, cardiometabolic risk in some populations. Although the risk-benefit tradeoff of using PrEP versus acquisition of HIV undoubtedly favors prevention at the population level, exploring the consequences of PrEP exposure on immune response and metabolism is important to individualizing care.

Results

PrEP exposure decreases mitochondrial respiration

To assess the effects of PrEP exposure on mitochondrial function, we obtained PBMCs from people without HIV and incubated these cells overnight with FTC or TDF, and measured real-time mitochondrial oxygen consumption rate (OCR) in live cells. Subsequent injections of oligomycin (ATP synthase inhibitor), carbonyl cyanide 4-(trifluoromethoxy) phenylhydrazone (FCCP) (mitochondrial uncoupler), and rotenone/antimycin A (complex I and II inhibitors) were used to assess mitochondrial basal and maximum respiration, spare respiratory capacity, ATP production, proton leak, and non-mitochondrial respiration (**Fig. 1A,B**) (10, 11). FCCP-induced maximal OCR and spare respiratory capacity, an indicator of a cell's ability to respond to energetic demand, were significantly decreased in PBMCs exposed to FTC and TDF, indicating mitochondrial dysfunction in PrEP-treated cells (**Fig. 1C**). We did not detect significant differences in measures of basal respiration, proton leak, or ATP-linked respiration in cells left unstimulated versus cells exposed to PrEP drugs. Although not significantly different among treatment groups, cells exposed to FTC and TDF tended to have reduced non-mitochondrial respiration levels (**Fig. 1C**). Overall, oxygen consumption rate kinetics were decreased in PrEP-treated PBMCs (**Fig.1B**).

We next asked whether PrEP exposure was sufficient to alter mitochondrial mass, as changes in mitochondrial content may affect cellular respiration(12). PBMCs were stained with MitoTracker Green, a green-fluorescent stain that localizes to mitochondria in live cells regardless of mitochondrial membrane potential. Monocytes exposed to TDF, and CD4+ and CD8+ T cells exposed overnight to FTC and TDF had significantly reduced mitochondrial mass, as assessed by MitoTracker Green staining (**Fig. 2A,B**). Monocyte-derived macrophages (MDMs) differentiated for 5 days in the presence of FTC and TDF also had reduced mitochondrial content compared to untreated cells (**Fig. 2A**). Altered mitochondrial function and morphology may lead to increased ROS production, further exacerbating oxidative stress(13). We detected significantly increased levels of intracellular ROS production in monocyte subsets exposed to FTC and TDF in whole blood directly *ex vivo* (**Fig. 2C**).

PrEP exposure increases lipid uptake by MDMs

To examine the consequences of PrEP exposure on macrophage phenotype and function, MDMs from participants without HIV were differentiated for 5 days in autologous serum in the presence of FTC and TDF. Intracellular lipid accumulation was increased in MDMs differentiated in the presence of both FTC and TDF (**Fig. 3A**). Consistent with alterations in lipid uptake, surface expression of lipid-binding scavenger receptors, CD36 and scavenger receptor-A (SR-A), was increased on MDMs differentiated in the presence of PrEP drugs.

ART use in PWH has been previously linked to dyslipidemia and altered lipid processing (14), however, the metabolic consequences of using ART for PrEP are unclear. MDMs obtained from people without HIV and differentiated in serum pooled from people without HIV, PWH on ART, or ART-naïve PWH displayed different patterns of lipid accumulation. MDMs differentiated in pooled serum from PWH on ART displayed significantly more intracellular lipid accumulation than MDMs differentiated in either serum pooled from people without HIV or ART-

naïve PWH. These findings may suggest that ART exposure could have adverse metabolic consequences *in vivo* in people with and without HIV.

Transcriptional profiles are altered in MDMs differentiated in the presence of PrEP

When compared to untreated MDMs, MDM differentiation in the presence of FTC and TDF resulted in distinct transcriptional profiles. We identified 888 differentially expressed genes (DEGs) in FTC-treated MDMs, and 829 DEGs in TDF-treated MDMs compared to gene expression in the control group. Additionally, we identified 568 DEGs comparing FTC and TDF treatment groups, indicating significant divergent effects of each drug on MDM transcript profiles. The top 50 DEGs for each treatment comparison are visualized as heatmaps in **Figure 4**. PrEP exposure altered numerous signaling pathways associated with mitochondrial dysfunction, inflammatory signaling, and lipid processing (**Supplemental Figure 1**). We identified differential expression of mitochondrial subunit genes (COX5A/B; COX6A1; NDUFB9; NDUFA12) and multiple genes involved in inflammation and immune responses (CCL3; CCR7; CXCL3; CXCR4; STAT2; MYD88; NLRP3; SOCS6; SOD2; ADORA1; CD48). We also found altered expression of numerous histone genes (e.g. HIST1H4; HIST2H2A; HIST2H2B; HIST1H3F; HIST1H1E) and genes involved in chromatin/nucleosome structure (e.g. NDC80; PRC1; CCNF; CCNB1; NUSAP1). A complete list of significantly altered genes among our treatment groups is provided in **Supplemental Table 1**. Network analysis revealed highly interconnected clusters of these histone and chromatin-related genes differentially expressed in MDMs exposed to PrEP (**Figure 5**).

MDMs differentiated in the presence of PrEP also displayed reduced expression of MERTK, a gene encoding a receptor that mediates engulfment and clearance of apoptotic cells(15). Clearance of apoptotic cells, or efferocytosis, by macrophages is important to inhibit inflammation and necrotic core formation in atherosclerotic plaques, and this mechanism is impaired in advanced atherosclerosis(16, 17). Decreased efferocytosis may also underlie

inflammation and tissue damage in other sites when apoptotic cells are inefficiently cleared and secondary necrosis occurs (18). To determine whether PrEP exposure altered efferocytosis capacity of MDMs, we incubated MDMs with apoptotic Jurkat cells labeled with a pH-sensitive fluorescent dye to assess phagocytic uptake by MDMs. MDMs differentiated in the presence of FTC and TDF displayed significantly less efferocytosis than control MDMs (**Fig. 6A,B**).

Lipids and inflammatory plasma biomarker levels are altered in individuals after initiating PrEP

To begin exploring *in vivo* consequences of PrEP use, we collected plasma from a convenience sampling of individuals before and after initiating a PrEP regimen (N=27; median= 7 months PrEP; mean= 9 months PrEP; range= 1.7 months – 2.6 years). Several plasma biomarkers were altered in the time period following PrEP initiation, including increased sVCAM1 and adiponectin levels (**Figure 7A**). Additionally, plasma levels of sVCAM1 were directly associated with adiponectin levels (**Supplemental Figure 2**). We also observed increased levels of intestinal fatty acid binding protein (I-FABP) that approached statistical significance. Further, LPS-binding protein (LBP) plasma levels were directly associated with sCD14, sTNFR1, and sTNFR2, and Zonulin plasma levels were directly associated with OxLDL in individuals after initiating PrEP (**Supplemental Figure 2**). Duration of PrEP use was directly associated with plasma CRP levels (**Supplemental Figure 2)**. *In vitro* exposure of human aortic endothelial cells (HAECs) to FTC and TDF resulted in increased levels of VCAM-1 mRNA, supporting our observation of increased plasma VCAM-1 in PrEP users (**Supplemental Figure 3**).

ART exposure contributes to altered lipid profiles in PWH, however the consequences of ART exposure on lipidomes of people without HIV have not been adequately explored. Lipidomic analyses on plasma samples from a subset individuals before and after PrEP exposure (N=15) demonstrated significantly increased concentrations of lipid species

PC(18:2/22:5), FFA(22:5), LCER(14:0), and DAG(16:1/22:6) following PrEP use ($p<0.05$ for all) (data not shown). We also observed increased total concentration of the hexosylceramide (HCER) lipid class (**Figure 7B**), and increased levels of the HCER lipid species HCER(16:0), HCER(20:0), HCER(24:0, and HCER(24:1) in individuals taking PrEP ($p<0.05$ for all) (**Figure 7C**).

Discussion

Much of the current knowledge regarding consequences of ART exposure was gained from studies in PWH. Suppressive ART significantly increases lifespans of PWH, but ART use can also alter metabolic profiles(19, 20) and contribute to CVD risk(21-25). ART initiation is associated with reduced systemic inflammation in PWH, although levels are often not reduced to levels observed in people without HIV(26). Persistent inflammation in PWH may be driven, at least in part, by ART's adverse effects on mitochondrial function(9). The immunologic consequences of ART use for PrEP in people without HIV have not been well characterized, however, initial studies have reported declines in kidney function and bone mineral density with long-term PrEP use (27-30). A recent study examining ART-related mitochondrial toxicity in HIV-exposed individuals prescribed a post-exposure prophylaxis (PEP) regimen, demonstrated mitochondrial toxicity after short-term ART use in the absence of HIV infection. Although PEP regimens using newer antiretrovirals, such as TDF + FTC, showed less mtDNA depletion than regimens that included AZT (31).

Here, we report several metabolic, transcriptional, and functional changes in immune cells following exposure to PrEP drugs. Overnight exposure to TDF or FTC resulted in overall decreased OCR in PBMCs, and significantly reduced maximal respiration and spare respiratory capacity. Further, exposure to TDF or FTC also resulted in decreased mitochondrial mass in monocytes and both CD4+ and CD8+ T cells, and increased ROS production from monocyte subsets. These findings demonstrate that exposure to TDF and FTC alters mitochondrial

function, potentially as a consequence of decreased mitochondrial mass. Previous work has shown that NRTI-mediated inhibition of DNA polymerase-γ leads to depletion of mitochondrial DNA levels and accumulation of mtDNA mutations, and subsequently mitochondrial dysfunction and altered energy production (32). Previous reports have also demonstrated NRTIs, such as TDF, FTC, and zidovudine, can alter mitochondrial dNTP pools and impair mitochondrial DNA replication (33), and also affect mitochondrial function via alterations in cellular metabolism and oxidative stress. Our current report is supportive of these previous findings, and further study is warranted to elucidate mechanisms underlying TDF- and FTC-induced mitochondrial dysfunction observed *in vitro* (34, 35).

We specifically explored the effects of PrEP exposure on MDMs, as these cells have key mitochondrial-dependent effector functions in tissues and are important in the development and progression of CVD. Monocytes migrate from the blood into tissue sites, where they differentiate into macrophages exhibiting a broad phenotypic range, driven by stimuli in the microenvironment (36-40). Here, we demonstrate MDMs differentiated in the presence of TDF or FTC internalize more lipids and have a decreased capacity to internalize apoptotic cells (efferocytosis). PrEP exposure also increased expression of the innate/lipid receptors CD36 and SR-A, providing one potential mechanism for enhanced lipid uptake. Interestingly, when MDMs from people without HIV were differentiated in the presence of serum pooled from PWH receiving a FTC/TDF/Raltegravir regimen, these cells displayed significantly increased intracellular lipid accumulation compared to MDMs differentiated in either pooled serum from people without HIV or pooled serum from ART-naïve PWH, despite the fact that sera from ART-naïve PWH typically contain high levels of inflammatory cytokines, microbial products, and HIV-1 itself (41-43). Our data would suggest the possibility that alterations in lipid uptake induced by factors in serum of PWH were more related to ART exposure than to the circulating pro-inflammatory cytokines. Further, exposure to TDF or FTC during MDM differentiation resulted in substantial changes in the transcriptional profiles of these cells. Expression of over 800

hundred genes were altered following exposure of MDMs to PrEP. Further, transcriptional network analyses demonstrated interconnected clusters of differentially expressed genes involved in mitochondrial dysfunction, immune regulation, and histone/chromatin modification. We also identified over 500 differentially expressed genes when comparing MDMs differentiated in either TDF or FTC, suggesting that although from the same class of ART, some of the mechanisms by which these drugs alter immune cell function are likely different. We did identify 126 genes that were similarly altered among TDF and FTC exposed MDMs, including CCL3, CCR7, COX5B, RUNX2, and STAT2. These *in vitro* results demonstrate that exposure to PrEP drugs can alter the transcriptional, metabolic, and functional capacity of immune cells. Future studies should also examine differential immune response to infection in MDMs exposed to PrEP, as alterations in immune signaling cascades may have important implications for the recognition and response to bacterial and viral ligands.

We also measured *in vivo* changes in lipid levels in individuals who were initiating PrEP. Notably, total HCER levels, as well as concentrations of multiple HCER lipid species, were increased with PrEP use. Ceramides, including HCERs, have been previously linked to cardiometabolic complications and insulin resistance (44-48). Furthermore, HCERs (22:0; 24:0; 24:1) were previously associated with hepatic inflammation and non-alcoholic steatohepatitis in obese adults (49), and we observed increased concentrations of these HCER species following PrEP initiation. Further studies exploring the changes in the lipidomes of PrEP users and the metabolic complications of ART should be considered.

Plasma biomarkers were also altered with PrEP use. Levels of VCAM-1, adiponectin, and I-FABP were increased in plasma samples following PrEP exposure. *In vitro* exposure of primary human aortic endothelial cells to FTC and TDF similarly resulted in increased expression of VCAM-1. Increased circulating concentrations of endothelial activation markers, such as VCAM-1 have been described in PWH, and are linked to chronic immune activation. I-FABP levels are indicative of gut epithelial barrier integrity, and are linked to mortality in PWH

(50, 51), and gastrointestinal side effects associated with PrEP initiation have been described (52). Unique characteristics, specific to individual PrEP users in this cohort, including lifestyle factors, underlying comorbidities, and/or coinfections, may influence levels of inflammatory markers and their changes over time, and we did not have access to detailed medical record information from this cohort. The need for well-designed trials exploring the immunologic and metabolic consequences of ART use in people without HIV are underscored by our results and the recent findings by Korencak et al, which demonstrated that exposure of immune cells to different classes of ART drugs, both *in vitro* and *in vivo*, resulted in changes in metabolic and functional signatures from these cells (35). Importantly, exposure to integrase inhibitors (dolutegravir and elvitegravir) resulted in decreased polyfunctionality of CD4+ T cells and instead promoted stress responses (increased TNF-α and ROS). In ART-treated women with HIV, monocyte mitochondrial and glycolytic dysfunction was associated with body composition (34), suggesting that future studies in PrEP users should also explore changes in body composition and mitochondrial function as well.

Exposure of immune cells to ART, as HIV-1 treatment or as PrEP, likely has important consequences on the metabolic and functional capacity of innate and adaptive immune cells, and may affect immune responses and cardiometabolic risk in both populations. The risk of taking PrEP versus the benefit of avoiding HIV acquisition clearly favors prevention, regardless of the off-target effects of ART exposure on immune cell function; yet, these findings merit further study to optimize PrEP methods. New PrEP formulations, including FTC and tenofovir alefenamide (DESCOVY®) and the long acting injectable PrEP cabotegravir are being administered for HIV prevention; the effects of these drugs on immune cells, the lipidome, and mitochondrial function should be explored (53). Further studies are needed to adequately understand the *in vivo* consequences of long-term PrEP exposure on immune cell mitochondrial function and gene expression, lipid metabolism, and risk for adverse health outcomes that may alter PrEP risk/benefit considerations.

Materials and Methods

Sample collection

Blood samples were collected in EDTA-containing vacutainer tubes (BD Biosciences) for PBMC isolation and whole blood stimulations. For serum collection, blood was drawn into serum separating tubes (SST, BD Biosciences) and centrifuged for 15 min at 800 x g. Study participants initiating PrEP (n=27) were enrolled at Case Western University following written informed consent. Longitudinal plasma samples were collected before and after initiation of PrEP (median= 7 months PrEP; mean= 9 months PrEP; range= 1.7 months – 2.6 years).

PBMC isolation and cell culture

PBMCs were freshly isolated from donors without HIV by centrifugation over Ficoll-Hypaque, and cultured in RPMI 1640 supplemented with 10% autologous serum. For differentiation of monocyte-derived macrophages (MDMs), donor PBMCs (2x10^6/mL) were cultured in Teflon wells (Savillex) for 5 days in RPMI 1640 supplemented with 20% autologous serum. On day 5, cells were removed from Teflon and MDMs were purified by adherence to plastic for 3 h. For MDM pooled serum experiments, PBMCs were isolated from donors without HIV (N=7) and differentiated in Teflon wells for 5 days in 20% serum pooled from donors without HIV, donors with HIV on ART (HIV-1 RNA <40 copies/mL), or ART-naïve donors with HIV. Human aortic endothelial cells (HAECs) were purchased from PromoCell, and grown in low serum endothelial cell growth medium with supplement mix (PromoCell).

Lyophilized FTC and TDF stocks were obtained from the AIDS-Reagent Repository, and solubilized in water. For *in vitro* PrEP experiments, PBMCs (1x10^6 cells/well) were exposed to FTC (1 uM) and TDF (1 uM) for 24 h, and monocyte-derived macrophages (MDMs) were differentiated for 5 days in the presence of FTC (0.1 uM) and TDF (0.1 uM). MDM morphology

had a healthier 'fried egg' appearance at the lower concentration of 0.1 μM for the longer period of time (5 days), compared to the higher concentration of 1 μM for the shorter period of time (24 h) for PBMC experiments. Clinically relevant concentrations were selected based on initial dose response assays (54-56). Cells maintained ~100% viability until >1000 μM drug exposure (24 h).

Flow cytometry

Cells harvested from Teflon were washed and blocked in 10% human AB serum (Sigma) for 60 min. MDMs were then stained for 30 min in the dark on ice, washed, and fixed in 1% paraformaldehyde. Monocytes and MDMs were identified by granularity, size, and surface expression of CD14 and CD16 (anti-CD14 pacific blue and anti-CD16 PE, BD Pharmingen). MDM scavenger receptor expression was measured using anti-CD36 (APC) (BD Pharmingen) and anti-SR-A (CD204, FITC) (Miltenyi Biotec). T cells were identified by granularity, size, and surface expression of CD3 (APC), CD4 (pacific blue), and CD8 (PerCP) (BD Pharmingen for all). For analysis of mitochondrial mass, cells were stained with MitoTracker green (200 nM, ThermoFisher) for 30 min at 37°C. To evaluate intracellular lipid accumulation, MDMs were stained with 0.25 ug/mL Bodipy 493/503 (Life Technologies) for 20 min in the dark at room temperature, and then analyzed by flow cytometry. Cells were analyzed using a Miltenyi MACSQuant Analyzer 10 flow cytometer, and MACSQuant analysis software. Statistical analysis was performed in GraphPad Prism 6, and paired t tests were used to compare flow cytometric data obtained from cells exposed to TDF or FTC and no drug controls.

Measurement of intracellular reactive oxygen species

CellROX Deep Red (ThermoFisher) is a cell permeable probe that exhibits excitation/emission maxima at ~640/665 upon oxidation by reactive oxygen species (ROS). To

measure ROS, whole blood from donors without HIV was exposed to FTC (1 uM) or TDF (1 uM) for 3 h, and then incubated with 5uM CellROX Deep Red at 37C for 30 min. Blood samples were then incubated for 15 min on ice with FACS Lysis buffer (BD Biosciences), and washed with flow cytometry wash buffer in preparation for flow cytometry analysis.

Soluble markers

Levels of the following inflammatory plasma biomarkers were measured by ELISA (R&D Systems unless stated otherwise): soluble CD14 (sCD14), tumor necrosis factor receptor (TNFR)-1, TNFR-2, vascular cell adhesion molecule (VCAM)-1, C-reactive protein (CRP), LPS-binding protein (LBP), intestinal fatty acid binding protein (I-FABP), zonulin (Promokine), and oxidized low density lipoprotein (OxLDL) (Mercodia). Paired t tests were used to compare biomarker levels before and after PrEP initiation. Spearman correlations are reported for relationships among plasma biomarker levels.

Metabolic analyses

Mitochondrial oxygen consumption rate (OCR) kinetics were measured on an Agilent XFp analyzer (N=7) using the Mito Stress Test kit (Agilent Technologies) as per manufacturer's protocol. Prior to the assay, Agilent XFp cell culture miniplates were coated with Cell-Tak (22.4 μg/mL) (Corning). PBMCs were exposed overnight to FTC (1 μM) or TDF (1 μM), centrifuged and resuspended in Agilent XF assay medium, and plated (500,000 cells/well) into Cell-Tak coated miniplates to adhere PBMCs for analysis by XFp analyzer. In this assay, subsequent injections of oligomycin (ATP synthase inhibitor), carbonyl cyanide 4-(trifluoromethoxy) phenylhydrazone (FCCP) (mitochondrial uncoupler), and rotenone/antimycin A (complex I and II inhibitors) are added to the assay media to assess mitochondrial function. Optimal cell density and FCCP concentration (1 μM) were selected based on initial titration and dose response

assays. Statistical and data analysis was performed using Seahorse XF Cell Mito Stress Test report generator and supported Wave software.

Efferocytosis assays

MDM efferocytosis activity was measured using apoptotic Jurkat cells labeled with pHrodo green (ThermoFisher), a pH sensitive dye that only fluoresces in the acidic environment of phagosomes. Jurkat cells were incubated with dexamethasone (100 uM) overnight, and induction of apoptosis was verified using the Dead Cell Apoptosis kit (ThermoFisher). Apoptotic Jurkat cells were washed with PBS and labeled with 20 ng/mL pHrodo green (ThermoFisher) for 30 min at room temperature. Labeled apoptotic cells were resuspended in culture medium and used immediately.

After 5 days of differentiation in the presence of FTC (0.1 uM) or TDF (0.1 uM), MDMs were plated in 12-well culture plates (3 X 10^5 MDMs/mL) and purified by adherence to plastic for 3 h. MDMs were re-supplemented with PrEP drugs and incubated overnight. pHrodo green-labeled apoptotic Jurkats were added to MDMs (4:1 Jurkat to MDM ratio), and incubated at 37C for 1.5 h. Apoptotic cell uptake was analyzed by flow cytometry and quantified by mean fluorescence intensity (MFI). For negative controls and background correction, MDMs were incubated on ice for 1.5 h with pHrodo green-labeled apoptotic Jurkat cells. Final reported fluorescence intensity was calculated by subtracting intensity of cells incubated at 0°C from cells incubated at 37°C. Paired t tests were used for statistical comparisons between no drug and FTC or TDF-exposed cells.

RNA isolation and transcriptomic analyses

Total MDM RNA was isolated using RNeasy RNA isolation kit (Qiagen). RNA-Seq libraries were prepared with standard TruSeq Stranded Total RNA (Ribo-Zero) kits (Illumina) or

Clontech Smart-Seq Ultra Low kits plus Nextera XT adaptors (Clontech) and sequenced using an Illumina HiSeq2500 instrument (2 x 125 cycle, 6-plex, 30M+ paired reads/sample), i.e. beyond the depth plateau necessary to fully characterize the transcriptome and capture information encoded by rarer alternative transcripts and isoforms. Our Bioconductor 'R' pipeline is data-type agnostic and was used to demultiplex, QC, align (UCSC Hg38 human reference), annotate, and count the transcripts. Differential expression analysis was performed using EdgeR and gene-by-gene contrasts (t- or F-test) between groups. A false discovery rate (FDR) of 5% was employed to correct for multiple testing. Pathway analyses were performed using gene set variation analysis (GSVA), gene sets from MSigDB, and Ingenuity Pathway analysis.

For HAEC qPCR analysis, iScript cDNA synthesis kit and iQ SYBR Green Supermix were used (BioRad). Paired t tests were used for statistical calculations. VCAM-1 transcript levels were analyzed using the following primer set: Forward-TTTGACAGGCTGGAGATAGACT; Reverse- TCAATGTGTAATTTAGCTCGGCA

Lipid measurement

Plasma lipids were analyzed using the direct infusion-tandem mass spectrometry (DI-MS/MS) Lipidyzer platform (Sciex, MA, USA) that identifies and quantifies ~1,100 biological lipids covering 13 lipid classes (i.e. free fatty acids, ceramides, hexosylceramides, diacylglycerols, triacylglycerols). The Lipidyzer platform methodology has been described in detail elsewhere (57), but briefly, lipids were extracted from 100 µL of plasma using a modified Bligh-Dyer method. Over 50 stable isotope labeled internal standards spanning all 13 lipid classes were added to each sample prior to extraction for accurate quantitation. Extracts were reconstituted in dichloromethane/methanol (1:1) and analyzed using DI-MS/MS with DMS separation. A Shimadzu LC system was used for automated infusion of each plasma extract and for pumping running and rinse solutions through the lines. Plasma extracts were infused into a 5500 QTRAP

MS/MS with SelexION DMS technology (Sciex) and lipid species were targeted and quantitated using optimized MS/MS transitions. Data were generated using the Lipidomics Workflow Manager software (Sciex). Data are reported as concentrations (μM) and relative fatty acid composition (mol%) of total lipid classes and individual lipid species. Paired t tests were used for comparison of plasma lipid concentrations in individuals before and after PrEP initiation. P values <0.05 were considered statistically significant.

Acknowledgements

We thank the Nutrient & Phytochemical Analytic Shared Resource at The Ohio State University Comprehensive Cancer Center, Columbus, OH for mass spectrometry services for lipidomics analyses. Research reported in this publication was supported by The Ohio State University Comprehensive Cancer Center and the National Institutes of Health under grant number P30 CA016058. Our friend and colleague Benigno Rodriguez M.D. contributed to this work, but passed away before it could be published.

Funding

This work was supported by the National Institutes of Health (R01HL134544 to N.F.)

Figure Legends

Figure 1. PrEP exposure alters mitochondrial function. A) Cellular oxygen consumption rate (OCR) kinetics were measured on an Agilent XFp extracellular flux analyzer. As indicated, sequential injections of oligomycin (ATP synthase inhibitor), carbonyl cyanide 4-(trifluoromethoxy) phenylhydrazone (FCCP) (mitochondrial uncoupler), and rotenone/antimycin A (complex I and II inhibitors) are added to the assay media to assess mitochondrial function. B) PBMCs were exposed to FTC (1 uM) or TDF (1 uM) for 24 h, plated into XFp microplates (500,000 cells/well), and overall OCR kinetics and effects of mitochondrial inhibitors on respiration are shown (+p,0.05, No Drug v FTC; *p<0.05, No Drug v TDF; n=6 donors) C) Basal and maximal respiration, spare respiratory capacity, proton leak, ATP-linked respiration, and non-mitochondrial respiration values were calculated using the Agilent Mito Stress Test report generator. (*p<0.05)

Figure 2. PrEP exposure alters mitochondrial mass measurements in PBMCs. PBMCs (1x10^6 cells/well) were cultured overnight in the presence of FTC (1 uM) or TDF (1 uM). Mitochondrial mass of A) monocytes and monocyte-derived macrophages (MDMs) and B) T cells was analyzed by flow cytometry following staining with MitoTracker green. (*p<0.05, **p<0.01) C) Intracellular ROS production of ART-exposed monocyte subsets was analyzed by flow cytometry following staining with CellROX Deep RED reagent.

Figure 3. MDMs differentiated in the presence of PrEP display increased lipid accumulation and scavenger receptor expression. A) Intracellular lipid accumulation was measured by flow cytometry following staining with Bodipy cell permeable dye. B) Scavenger receptors CD36 and SR-A were measured by flow cytometry (*p<0.05, **p<0.01). C) PBMCs from people without HIV were differentiated in serum pooled from donors without HIV, donors with HIV on ART (HIV-1 RNA < 40 copies/mL), and ART-naïve donors with HIV. MDM lipid accumulation was assessed by flow cytometry analysis of Bodipy staining intensity.

Antimicrobial Agents and Chemotherapy

Figure 4. MDMs exposed to PrEP have altered gene expression profiles. Transcript analysis identified differentially expressed genes among MDMs from people without HIV (n=5) differentiated in the presence of medium alone or medium containing FTC (0.1 μM) or TDF (0.1 μM). The top 50 significantly differentially expressed genes (DEGs) are visualized as heatmaps, and the data are arranged by p-value and log fold change (LogFC).

Figure 5. Integrative network analyses of differentially expressed genes ($p<0.025$) in PrEP-exposed MDMs. Linkages among DEGs are displayed, and nodes demonstrating the most highly interconnected pathways are labeled (Pearson correlation coefficients). Red circles indicate increased gene expression, and blue circles indicated decreased gene expression.

Figure 6. PrEP exposure decreases MDM efferocytosis capacity. MDMs were exposed to pHrodo green-labeled apoptotic Jurkat cells (4:1 Jurkat to MDM) for 1.5 h at 37C. Apoptotic cell uptake was analyzed by flow cytometry. A) Representative histogram overlays; red line is MDMs incubated at 0C under indicated exposure condition. B) Summary data reporting percentage MDMs that have internalized apoptotic cells. (*$p<0.05$)

Figure 7. Plasma inflammatory biomarker levels and lipid concentrations are altered following initiation of PrEP. Plasma samples were collected from people without HIV before and after initiating ART as pre-exposure prophylaxis (PrEP). Levels of plasma biomarkers including A) VCAM-1 (ng/mL), adiponectin (ng/mL), and I-FABP (ng/mL) were measured by ELISA at pre- and post-PrEP initiation. The average duration of PrEP use among the subjects was 9 months. B) To assess lipid content, plasma samples were analyzed using direct infusion-

tandem mass spectrometry (DI-MS/MS) Lipidyzer platform. Concentrations of total HCER levels and C) individual HCER species are displayed. (*p<0.05)

References

1. Fauci AS, Redfield RR, Sigounas G, Weahkee MD, Giroir BP. 2019. Ending the HIV Epidemic: A Plan for the United States. JAMA doi:10.1001/jama.2019.1343.
2. Grant RM, Lama JR, Anderson PL, McMahan V, Liu AY, Vargas L, Goicochea P, Casapia M, Guanira-Carranza JV, Ramirez-Cardich ME, Montoya-Herrera O, Fernandez T, Veloso VG, Buchbinder SP, Chariyalertsak S, Schechter M, Bekker LG, Mayer KH, Kallas EG, Amico KR, Mulligan K, Bushman LR, Hance RJ, Ganoza C, Defechereux P, Postle B, Wang F, McConnell JJ, Zheng JH, Lee J, Rooney JF, Jaffe HS, Martinez AI, Burns DN, Glidden DV, iPrEx Study T. 2010. Preexposure chemoprophylaxis for HIV prevention in men who have sex with men. N Engl J Med 363:2587-99.
3. Martin JL, Brown CE, Matthews-Davis N, Reardon JE. 1994. Effects of antiviral nucleoside analogs on human DNA polymerases and mitochondrial DNA synthesis. Antimicrob Agents Chemother 38:2743-9.
4. Kakuda TN. 2000. Pharmacology of nucleoside and nucleotide reverse transcriptase inhibitor-induced mitochondrial toxicity. Clin Ther 22:685-708.
5. Miro O, Lopez S, Pedrol E, Rodriguez-Santiago B, Martinez E, Soler A, Milinkovic A, Casademont J, Nunes V, Gatell JM, Cardellach F. 2003. Mitochondrial DNA depletion and respiratory chain enzyme deficiencies are present in peripheral blood mononuclear cells of HIV-infected patients with HAART-related lipodystrophy. Antivir Ther 8:333-8.
6. McComsey GA, Walker UA. 2004. Role of mitochondria in HIV lipoatrophy: insight into pathogenesis and potential therapies. Mitochondrion 4:111-8.
7. Aon MA, Bhatt N, Cortassa SC. 2014. Mitochondrial and cellular mechanisms for managing lipid excess. Front Physiol 5:282.
8. Koh EH, Park JY, Park HS, Jeon MJ, Ryu JW, Kim M, Kim SY, Kim MS, Kim SW, Park IS, Youn JH, Lee KU. 2007. Essential role of mitochondrial function in adiponectin synthesis in adipocytes. Diabetes 56:2973-81.
9. Lopez-Armada MJ, Riveiro-Naveira RR, Vaamonde-Garcia C, Valcarcel-Ares MN. 2013. Mitochondrial dysfunction and the inflammatory response. Mitochondrion 13:106-18.
10. Wills LP, Beeson GC, Hoover DB, Schnellmann RG, Beeson CC. 2015. Assessment of ToxCast Phase II for Mitochondrial Liabilities Using a High-Throughput Respirometric Assay. Toxicological sciences : an official journal of the Society of Toxicology 146:226-234.
11. Sanuki Y, Araki T, Nakazono O, Tsurui K. 2017. A rapid mitochondrial toxicity assay utilizing rapidly changing cell energy metabolism. The Journal of Toxicological Sciences 42:349-358.
12. Brand MD, Nicholls DG. 2011. Assessing mitochondrial dysfunction in cells. The Biochemical journal 435:297-312.

13. Nagdas S, Kashatus DF. 2017. The Interplay between Oncogenic Signaling Networks and Mitochondrial Dynamics. Antioxidants (Basel, Switzerland) 6:33.
14. Lake JE, Currier JS. 2013. Metabolic disease in HIV infection. The Lancet Infectious Diseases 13:964-975.
15. Scott RS, McMahon EJ, Pop SM, Reap EA, Caricchio R, Cohen PL, Earp HS, Matsushima GK. 2001. Phagocytosis and clearance of apoptotic cells is mediated by MER. Nature 411:207-211.
16. Tabas I. 2005. Consequences and Therapeutic Implications of Macrophage Apoptosis in Atherosclerosis. Arteriosclerosis, Thrombosis, and Vascular Biology 25:2255-2264.
17. Schrijvers DM, De Meyer GRY, Herman AG, Martinet W. 2007. Phagocytosis in atherosclerosis: Molecular mechanisms and implications for plaque progression and stability. Cardiovascular Research 73:470-480.
18. Silva MT. 2010. Secondary necrosis: The natural outcome of the complete apoptotic program. FEBS Letters 584:4491-4499.
19. Lake JE, Currier JS. 2013. Metabolic disease in HIV infection. Lancet Infect Dis 13:964-75.
20. Willig AL, Overton ET. 2014. Metabolic Consequences of HIV: Pathogenic Insights. Curr HIV/AIDS Rep doi:10.1007/s11904-013-0191-7.
21. d'Arminio A, Sabin CA, Phillips AN, Reiss P, Weber R, Kirk O, El-Sadr W, De Wit S, Mateu S, Petoumenos K, Dabis F, Pradier C, Morfeldt L, Lundgren JD, Friis-Moller N. 2004. Cardio- and cerebrovascular events in HIV-infected persons. Aids 18:1811-7.
22. Kaplan RC, Kingsley LA, Gange SJ, Benning L, Jacobson LP, Lazar J, Anastos K, Tien PC, Sharrett AR, Hodis HN. 2008. Low CD4+ T-cell count as a major atherosclerosis risk factor in HIV-infected women and men. Aids 22:1615-24.
23. Mangili A, Gerrior J, Tang AM, O'Leary DH, Polak JK, Schaefer EJ, Gorbach SL, Wanke CA. 2006. Risk of cardiovascular disease in a cohort of HIV-infected adults: a study using carotid intima-media thickness and coronary artery calcium score. Clin Infect Dis 43:1482-9.
24. Mooser V. 2003. Atherosclerosis and HIV in the highly active antiretroviral therapy era: towards an epidemic of cardiovascular disease? Aids 17 Suppl 1:S65-9.
25. Periard D, Cavassini M, Taffe P, Chevalley M, Senn L, Chapuis-Taillard C, de Valliere S, Hayoz D, Tarr PE. 2008. High prevalence of peripheral arterial disease in HIV-infected persons. Clin Infect Dis 46:761-7.
26. Funderburg NT. 2014. Markers of coagulation and inflammation often remain elevated in ART-treated HIV-infected patients. Current opinion in HIV and AIDS 9:80-86.
27. Gandhi M, Glidden DV, Mayer K, Schechter M, Buchbinder S, Grinsztejn B, Hosek S, Casapia M, Guanira J, Bekker L-G, Louie A, Horng H, Benet LZ, Liu A, Grant RM. 2016. Association of age, baseline kidney function, and medication exposure with declines in creatinine clearance on pre-exposure prophylaxis: an observational cohort study. The lancet HIV 3:e521-e528.
28. Mulligan K, Glidden DV, Anderson PL, Liu A, McMahan V, Gonzales P, Ramirez-Cardich ME, Namwongprom S, Chodacki P, de Mendonca LMC, Wang F, Lama JR, Chariyalertsak S, Guanira JV, Buchbinder S, Bekker L-G, Schechter M, Veloso VG, Grant RM, Preexposure Prophylaxis Initiative Study T. 2015. Effects of Emtricitabine/Tenofovir on Bone Mineral Density in HIV-Negative Persons in a Randomized, Double-Blind, Placebo-Controlled Trial. Clinical infectious diseases : an official publication of the Infectious Diseases Society of America 61:572-580.
29. Tang EC, Vittinghoff E, Anderson PL, Cohen SE, Doblecki-Lewis S, Bacon O, Coleman ME, Buchbinder SP, Chege W, Kolber MA, Elion R, Shlipak M, Liu AY. 2018. Changes in Kidney Function Associated With Daily Tenofovir Disoproxil Fumarate/Emtricitabine for HIV Preexposure Prophylaxis Use in the United States Demonstration Project. Journal of acquired immune deficiency syndromes (1999) 77:193-198.

30. Martin M, Vanichseni S, Suntharasamai P, Sangkum U, Mock PA, Gvetadze RJ, Curlin ME, Leethochawalit M, Chiamwongpaet S, Cherdtrakulkiat T, Anekvorapong R, Leelawiwat W, Chantharojwong N, McNicholl JM, Paxton LA, Kittimunkong S, Choopanya K, Group ftBTS. 2014. Renal Function of Participants in the Bangkok Tenofovir Study—Thailand, 2005–2012. Clinical Infectious Diseases 59:716-724.
31. Bañó M, Morén C, Barroso S, Juárez DL, Guitart-Mampel M, González-Casacuberta I, Canto-Santos J, Lozano E, León A, Pedrol E, Miró Ò, Tobías E, Mallolas J, Rojas JF, Cardellach F, Martínez E, Garrabou G. 2020. Mitochondrial Toxicogenomics for Antiretroviral Management: HIV Post-exposure Prophylaxis in Uninfected Patients. Frontiers in genetics 11:497-497.
32. Payne BAI, Wilson IJ, Hateley CA, Horvath R, Santibanez-Koref M, Samuels DC, Price DA, Chinnery PF. 2011. Mitochondrial aging is accelerated by anti-retroviral therapy through the clonal expansion of mtDNA mutations. Nature genetics 43:806-810.
33. Chen X, Castillo-Mancilla JR, Seifert SM, McAllister KB, Zheng J-H, Bushman LR, MaWhinney S, Anderson PL. 2016. Analysis of the Endogenous Deoxynucleoside Triphosphate Pool in HIV-Positive and -Negative Individuals Receiving Tenofovir-Emtricitabine. Antimicrobial Agents and Chemotherapy 60:5387-5392.
34. Willig AL, Kramer PA, Chacko BK, Darley-Usmar VM, Heath SL, Overton ET. 2017. Monocyte bioenergetic function is associated with body composition in virologically suppressed HIV-infected women. Redox biology 12:648-656.
35. Korencak M, Byrne M, Richter E, Schultz BT, Juszczak P, Ake JA, Ganesan A, Okulicz JF, Robb ML, de Los Reyes B, Winning S, Fandrey J, Burgess TH, Esser S, Michael NL, Agan BK, Streeck H. 2019. Effect of HIV infection and antiretroviral therapy on immune cellular functions. JCI insight 4:e126675.
36. Xu S, Huang Y, Xie Y, Lan T, Le K, Chen J, Chen S, Gao S, Xu X, Shen X, Huang H, Liu P. 2010. Evaluation of foam cell formation in cultured macrophages: an improved method with Oil Red O staining and DiI-oxLDL uptake. Cytotechnology 62:473-481.
37. Fayad ZA, Swirski FK, Calcagno C, Robbins CS, Mulder W, Kovacic JC. 2018. Monocyte and Macrophage Dynamics in the Cardiovascular System: JACC Macrophage in CVD Series (Part 3). Journal of the American College of Cardiology 72:2198-2212.
38. Lavine KJ, Pinto AR, Epelman S, Kopecky BJ, Clemente-Casares X, Godwin J, Rosenthal N, Kovacic JC. 2018. The Macrophage in Cardiac Homeostasis and Disease: JACC Macrophage in CVD Series (Part 4). Journal of the American College of Cardiology 72:2213-2230.
39. Moore KJ, Koplev S, Fisher EA, Tabas I, Björkegren JLM, Doran AC, Kovacic JC. 2018. Macrophage Trafficking, Inflammatory Resolution, and Genomics in Atherosclerosis: JACC Macrophage in CVD Series (Part 2). Journal of the American College of Cardiology 72:2181-2197.
40. Williams JW, Giannarelli C, Rahman A, Randolph GJ, Kovacic JC. 2018. Macrophage Biology, Classification, and Phenotype in Cardiovascular Disease: JACC Macrophage in CVD Series (Part 1). Journal of the American College of Cardiology 72:2166-2180.
41. Roberts L, Passmore J-AS, Williamson C, Little F, Bebell LM, Mlisana K, Burgers WA, van Loggerenberg F, Walzl G, Djoba Siawaya JF, Karim QA, Karim SSA. 2010. Plasma cytokine levels during acute HIV-1 infection predict HIV disease progression. AIDS (London, England) 24:819-831.
42. Funderburg NT, Andrade A, Chan ES, Rosenkranz SL, Lu D, Clagett B, Pilch-Cooper HA, Rodriguez B, Feinberg J, Daar E, Mellors J, Kuritzkes D, Jacobson JM, Lederman MM. 2013. Dynamics of Immune Reconstitution and Activation Markers in HIV+ Treatment-Naïve Patients Treated with Raltegravir, Tenofovir Disoproxil Fumarate and Emtricitabine. PLOS ONE 8:e83514.
43. Marchetti G, Tincati C, Silvestri G. 2013. Microbial translocation in the pathogenesis of HIV infection and AIDS. Clinical microbiology reviews 26:2-18.

44. Zhao H, Przybylska M, Wu I-H, Zhang J, Siegel C, Komarnitsky S, Yew NS, Cheng SH. 2007. Inhibiting Glycosphingolipid Synthesis Improves Glycemic Control and Insulin Sensitivity in Animal Models of Type 2 Diabetes. Diabetes 56:1210-1218.
45. Chavez JA, Siddique MM, Wang ST, Ching J, Shayman JA, Summers SA. 2014. Ceramides and glucosylceramides are independent antagonists of insulin signaling. The Journal of biological chemistry 289:723-734.
46. Bozic J, Markotic A, Cikes-Culic V, Novak A, Borovac JA, Vucemilovic H, Trgo G, Ticinovic Kurir T. 2018. Ganglioside GM3 content in skeletal muscles is increased in type 2 but decreased in type 1 diabetes rat models: Implications of glycosphingolipid metabolism in pathophysiology of diabetes. Journal of Diabetes 10:130-139.
47. Chew WS, Torta F, Ji S, Choi H, Begum H, Sim X, Khoo CM, Khoo EYH, Ong W-Y, Van Dam RM, Wenk MR, Tai ES, Herr DR. 2019. Large-scale lipidomics identifies associations between plasma sphingolipids and T2DM incidence. JCI insight 5:e126925.
48. Peterson LR, Xanthakis V, Duncan MS, Gross S, Friedrich N, Völzke H, Felix SB, Jiang H, Sidhu R, Nauck M, Jiang X, Ory DS, Dörr M, Vasan RS, Schaffer JE. 2018. Ceramide Remodeling and Risk of Cardiovascular Events and Mortality. Journal of the American Heart Association 7:e007931.
49. Apostolopoulou M, Gordillo R, Koliaki C, Gancheva S, Jelenik T, De Filippo E, Herder C, Markgraf D, Jankowiak F, Esposito I, Schlensak M, Scherer PE, Roden M. 2018. Specific Hepatic Sphingolipids Relate to Insulin Resistance, Oxidative Stress, and Inflammation in Nonalcoholic Steatohepatitis. Diabetes Care 41:1235-1243.
50. Hunt PW, Sinclair E, Rodriguez B, Shive C, Clagett B, Funderburg N, Robinson J, Huang Y, Epling L, Martin JN, Deeks SG, Meinert CL, Van Natta ML, Jabs DA, Lederman MM. 2014. Gut epithelial barrier dysfunction and innate immune activation predict mortality in treated HIV infection. The Journal of infectious diseases 210:1228-1238.
51. Sandler NG, Wand H, Roque A, Law M, Nason MC, Nixon DE, Pedersen C, Ruxrungtham K, Lewin SR, Emery S, Neaton JD, Brenchley JM, Deeks SG, Sereti I, Douek DC, Group ISS. 2011. Plasma levels of soluble CD14 independently predict mortality in HIV infection. J Infect Dis 203:780-90.
52. Dubé MP, Park SY, Ross H, Love TMT, Morris SR, Lee HY. 2018. Daily HIV pre-exposure prophylaxis (PrEP) with tenofovir disoproxil fumarate-emtricitabine reduced Streptococcus and increased Erysipelotrichaceae in rectal microbiota. Scientific reports 8:15212-15212.
53. Clement ME, Kofron R, Landovitz RJ. 2020. Long-acting injectable cabotegravir for the prevention of HIV infection. Curr Opin HIV AIDS 15:19-26.
54. Stray KM, Park Y, Babusis D, Callebaut C, Cihlar T, Ray AS, Perron M. 2017. Tenofovir alafenamide (TAF) does not deplete mitochondrial DNA in human T-cell lines at intracellular concentrations exceeding clinically relevant drug exposures. Antiviral Research 140:116-120.
55. Callebaut C, Stepan G, Tian Y, Miller MD. 2015. In Vitro Virology Profile of Tenofovir Alafenamide, a Novel Oral Prodrug of Tenofovir with Improved Antiviral Activity Compared to That of Tenofovir Disoproxil Fumarate. Antimicrobial agents and chemotherapy 59:5909-5916.
56. Wang L. 2004. Pharmacokinetic and Pharmacodynamic Characteristics of Emtricitabine Support Its Once Daily Dosing for the Treatment of HIV Infection. AIDS Research and Human Retroviruses 20:1173-1182.
57. Ubhi BK. 2018. Direct Infusion-Tandem Mass Spectrometry (DI-MS/MS) Analysis of Complex Lipids in Human Plasma and Serum Using the LipidyzerTM Platform Clinical Metabolomics:227-236.

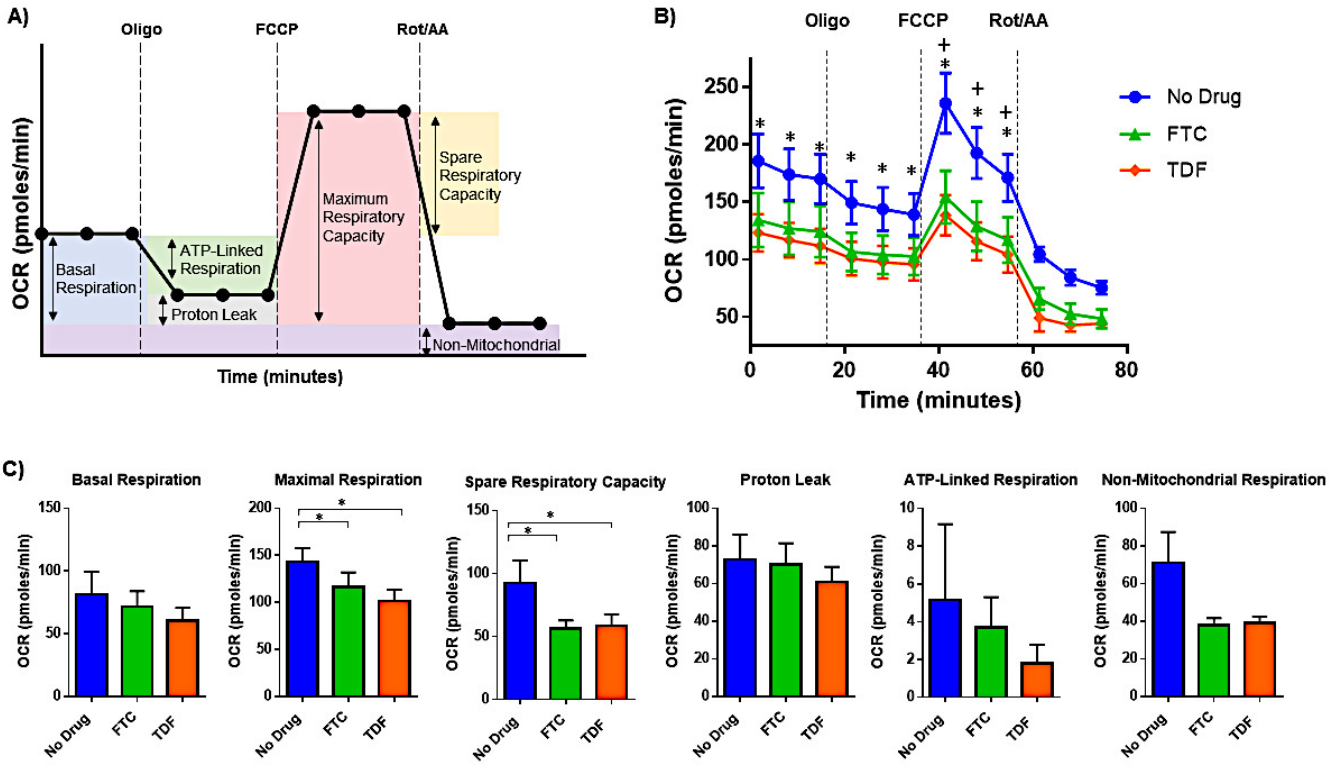

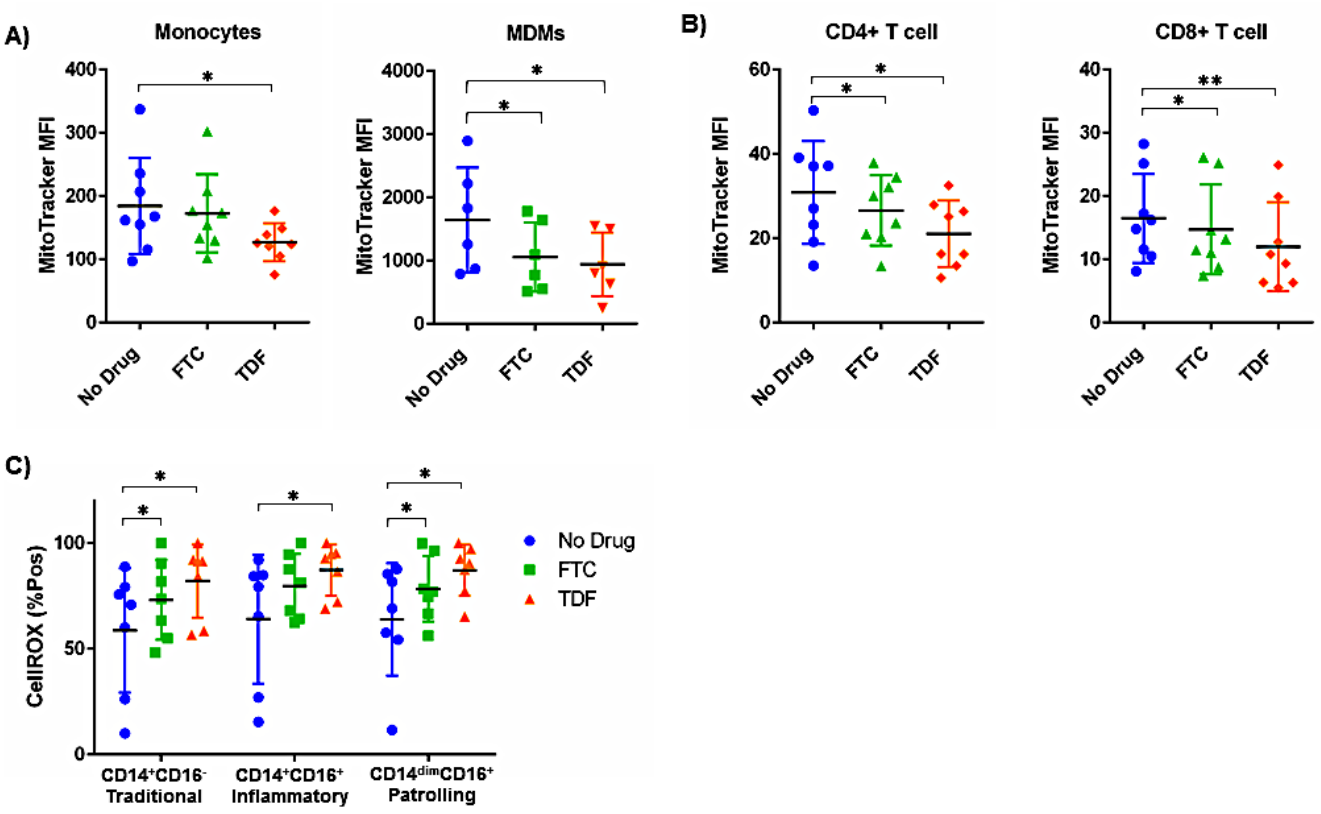

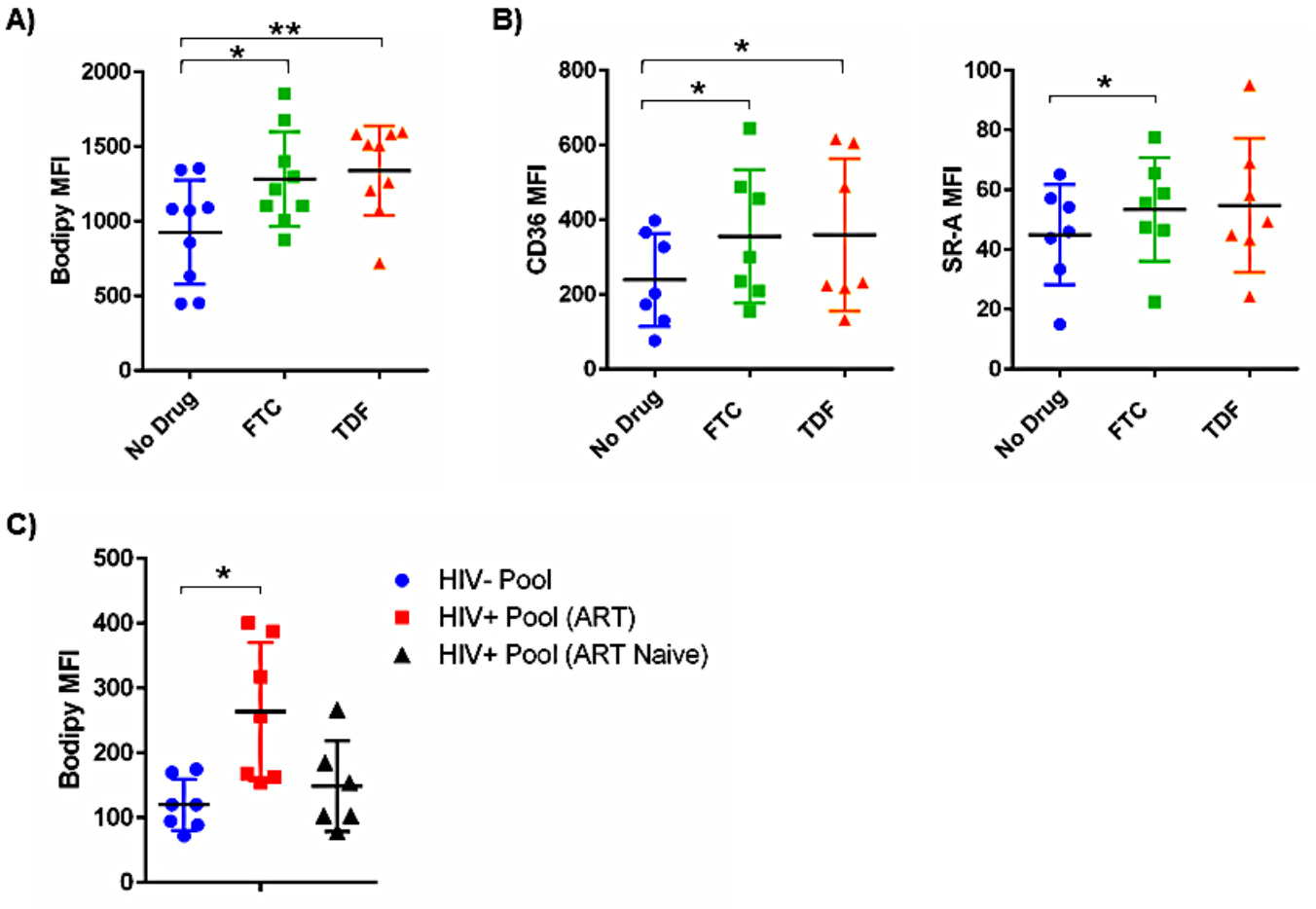

Antimicrobial Agents and Chemotherapy

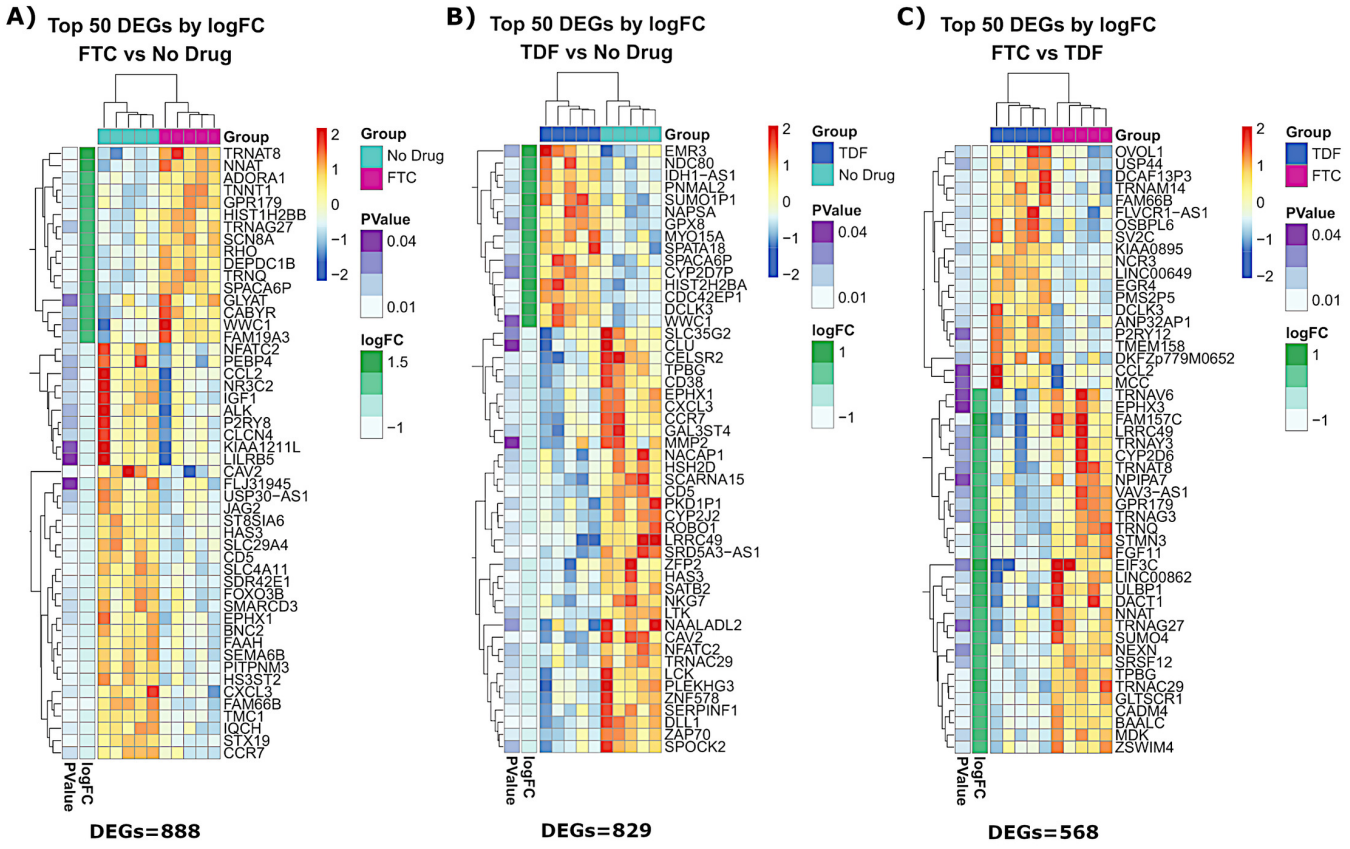

Antimicrobial Agents and Chemotherapy